Enhanced Motorcycle Roll Stability by use of a Reaction Wheel Actuator

Georgios Mavros
Aeronautical and Automotive Engineering department, Loughborough University

AAE, Loughborough University
Loughborough, Leicestershire, LE11 3TU, UK
Phone: (0044(0)1509) 227273
Fax: (0044(0)1509) 227275
E-mail: g.mavros@lboro.ac.uk

The paper presents a preliminary study on the use of the reaction wheel for improving the roll stability of motorcycles. The development of the controller is based on the dynamics of the reaction wheel pendulum. A feedback linearization approach is employed for the control of the reaction wheel pendulum and the resulting controller is subsequently implemented in a 12 degree-of-freedom non-linear motorcycle model. Simulations reveal the effectiveness of the controller, as well as some problems related to unrealistic power requirements and gyroscopic effects of the reaction wheel during cornering. The latter are treated by introduction of a moving roll-angle reference, while some proposals for reducing the required power to realistic levels are also discussed.

Topics/Vehicle Dynamics, Vehicle Control, Motorcycle

1. INTRODUCTION

The dynamic behaviour of motorcycles has been thoroughly studied in the past. Some important findings are highlighted here, in order to provide the necessary background for the present study.

Motorcycle motion is highly non-linear and, typically, a multi-body formulation approach is essential in order to capture the complex dynamic interactions. The minimum requirements for a linear treatment of motorcycle dynamics are summarized in [1]. Non-linear multi-body models including wheel and suspension dynamics are presented in [2-5]. In [2] the constrained Lagrange equations, whereby joint reactions are represented by Lagrange multipliers are used for the derivation of the non-linear equations of motion. The model possesses 11 DOF (degrees-of-freedom) and does not include driver lean or frame flexibility. In [4], [5] multi-DOF models are developed with the aid of the multi-body code AutoSim®. These models include frame and suspension flexibilities as well as rider lateral and roll motions. When linearising non-linear models about straight-line operating points, there appear to be two distinct families of eigenvectors, signifying the in-plane and out of plane modes. These families are decoupled in straight line but intertwined in steady-state cornering [3], [4]. There is a strong dependency of the out-of-plane modes and their corresponding eigenvalues on speed and some of them can become lightly damped or even unstable within certain speed regions [3], [4], [5]. Characterisation of the modes is based on the relative presence of certain DOFs in the eigenvectors. The capsize mode is described as a motion resembling that of an inverted pendulum or capsizing ship [4]. This mode is unstable at low speeds but stabilizes at higher speeds [3], [4]. Other important modes include the weave and wobble, which are both oscillatory and speed-dependent and involve a significant contribution from the steering DOF. It is important to note that when cornering at large roll (lean) angles, the low speed divergent instability (capsize) tends to become more severe and requires additional concentration from the driver [4].

In terms of rider control, the steering torque and rider body lean torque are established as primary control inputs, with the former being much more effective [4], [6]. Significant improvements in capsize stability result from feeding the roll-angle error back into the steering torque input [4].

The work presented herein focuses on improving the straight-line capsize stability of a motorcycle using the reaction wheel actuator. At the same time, the method proposed assists the rider in maintaining stability when cornering at large roll-angles and may provide the basis for a motorcycle ride-by-wire system.

2. DEVELOPMENT OF THE CONTROLLER

The reaction wheel is a simple actuator used frequently for the direction/orientation of aerospace structures, such as satellites [7]. It consists of an electric motor connected to a rotational inertia. The motor provides a moment couple by accelerating the inertia. A common application of the reaction wheel involves the swing-up and balancing control of the inverted pendulum [8], [9]. In the following section, the base-line controller is developed by exploiting the resemblance of the low-speed capsize dynamics of the motorcycle to the dynamics of the inverted pendulum.

2.1 The Reaction Wheel Pendulum

The controlled pendulum is developed in-line with the feedback linearization scheme presented in [8] for balancing the inverted pendulum. The approach is based on Isidori [10] and it ensures stabilisation of the inverted pendulum for any angle above the horizontal, i.e. angles between $\pm\pi/2$. For completeness, the development of the controller is briefly presented here.

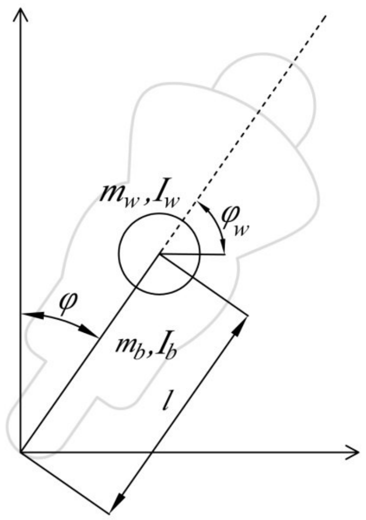

Fig. 1 The inverted pendulum with the reaction wheel

A schematic of the inverted pendulum with the reaction wheel attached is provided in Fig. 1. In this particular case the position of the reaction wheel is chosen to coincide with the centre of mass of the motorcycle including the driver, but this is an arbitrary choice and it is not restrictive. Using Lagrange, the equations of motion of the pendulum are easily derived as follows:

$$(I_b + I_w + (m_b + m_w)l^2)\ddot{\varphi} + I_w\ddot{\varphi}_w - g(m_b + m_w)l \sin\varphi = 0 \quad (1)$$

$$I_w\ddot{\varphi} + I_w\ddot{\varphi}_w = \tau \quad (2)$$

where τ is the torque of the motor and g the acceleration of gravity.

In order to write the equations in non-linear state-space form the states considered are the angle of the pendulum, $x_1 = \varphi$, its rate of change, $x_2 = \dot{\varphi}$ and the angular speed of the reaction wheel with respect to the pendulum, $x_3 = \dot{\varphi}_w$. The equations are written as:

$$\dot{\boldsymbol{x}} = f(\boldsymbol{x}) + g(\boldsymbol{x})\tau \quad (3)$$

where

$$\boldsymbol{x} = [x_1\ x_2\ x_3]^T \quad (4)$$

and

$$f(\boldsymbol{x}) = \begin{bmatrix} x_2 \\ \frac{I_w}{detD} g(m_b + m_w)l \sin(x_1) \\ -\frac{I_w}{detD} g(m_b + m_w)l \sin(x_1) \end{bmatrix} \quad (5)$$

$$g(\boldsymbol{x}) = \begin{bmatrix} 0 \\ -\frac{I_w}{detD} \\ \frac{(I_b + I_w + (m_b + m_w)l^2)}{detD} \end{bmatrix} \quad (6)$$

$$detD = (I_b + I_w + (m_b + m_w)l^2)I_w - I_w^2 \quad (7)$$

To proceed with feedback linearization, an output equation is defined as follows:

$$y = h(\boldsymbol{x}) = (I_b + I_w + (m_b + m_w)l^2)x_2 + I_w x_3 \quad (8)$$

By calculating the 1st, 2nd and 3rd time-derivatives of the output defined in eq. (8), it can be shown that the system has a relative degree of three with respect to the output, y [8]. In particular:

$$\dot{y} = (m_b + m_w)lg \sin(x_1)$$
$$\ddot{y} = L_f^2 h \quad (9)$$
$$\dddot{y} = L_f^3 h + L_g L_f^2 h\tau$$

where

$$L_f^2 h = (m_b + m_w)lg \cos(x_1)\, x_2$$
$$L_f^3 h = -(m_b + m_w)lg \sin(x_1)\, x_2^2 + (m_b + m_w)^2 l^2 g^2 I_w \cos(x_1)\sin(x_1)/detD \quad (10)$$
$$L_g L_f^2 h = I_w(m_b + m_w)lg \cos(x_1)/detD$$

New state variables are defined as follows [8]:

$$\sigma_1 = (I_b + I_w + (m_b + m_w)l^2)x_2 + I_w x_3$$
$$\sigma_2 = (m_b + m_w)lg \sin(x_1) \quad (11)$$
$$\sigma_3 = (m_b + m_w)lg \cos(x_1)\, x_2$$

With the aid of the variables defined in eq. (11), the system can now be written as:

$$\dot{\sigma}_1 = \sigma_2$$
$$\dot{\sigma}_2 = \sigma_3 \quad (12)$$
$$\dot{\sigma}_3 = u$$

Where the relationship between the input, u, and the torque, τ, is given by the following equation [8]:

$$\tau = \left(1/L_g L_f^2 h\right)\left(u - L_f^3 h\right) \quad (13)$$

It is now possible to define the control input, u, for the system defined by eq. (12), as follows:

$$u = -\boldsymbol{k} \cdot \boldsymbol{\sigma} \tag{14}$$

The final non-linear controller consists of the linear law (14), applied to the states, $\boldsymbol{\sigma}$, that are related to the states, $\boldsymbol{x}$, through the transformation (11). The actual control torque, τ, is given by eq. (13).

2.2 Pendulum Simulation Results

The size and inertia of the pendulum are set so that they represent those of the actual motorcycle described later in the paper. Basic properties are given in table 1.

Table 1 Pendulum Parameters

Pendulum (motorcycle) mass	m_b	276.98 kg
Reaction wheel mass	m_w	12.33 kg
Pendulum (motorcycle) roll moment of inertia	I_b	32.00 kgm^2
Reaction wheel roll moment of inertia	I_w	6.17x10^{-2} kgm^2
Length of pendulum (height of c.g.)	l	0.636 m

The gain, $\boldsymbol{k}$, is set so that the linear system (12) in $\boldsymbol{\sigma}$ coordinates has closed loop poles at -6 and a complex pair at $-6 \pm 5.29i$. For the parameters included in Table 1, this requirement results in the gain vector:

$$\boldsymbol{k} = [k_1\ k_2\ k_3] = [383.9\ 136.0\ 18.0] \tag{15}$$

With the control law specified, a particularly interesting case-study is simulated whereby the pendulum rests initially in the inverted unstable equilibrium position and an external disturbance is applied. The disturbance corresponds to a lateral acceleration applied at the centre of mass of the motorcycle, or alternatively, equivalent lateral tyre forces applied at the tyre contact patches. The lateral acceleration is represented by a ramp starting from zero, increasing up to 0.8 g in 2 seconds and remaining equal to 0.8 g thereafter. The response of the system is illustrated in Fig. 2.

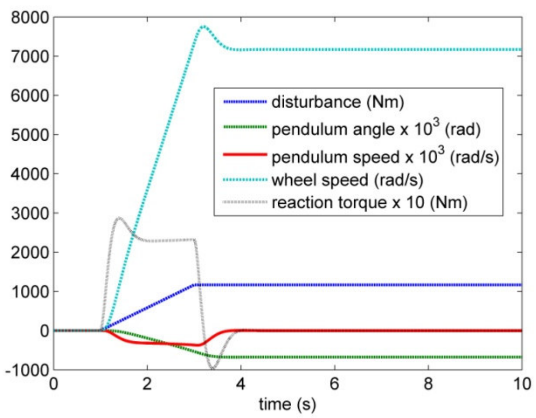

Fig. 2 Controlled pendulum response

Under the action of the disturbance, the pendulum balances at an angle of approximately -0.675 rad. This angle generates a gravitational moment opposing the one due to the disturbance and can be easily calculated as equal to $\tan^{-1} 0.8$, by taking a steady-state equilibrium of moments at a lateral acceleration of 0.8 g. At steady-state the reaction wheel torque is zero. Combining eq. (10), (11), (13), (14) with $\tau = 0$ and observing that x_2 and σ_3 must also be zero, it is possible to calculate the reaction wheel speed error, Δx_3, corresponding to the angle $x_1 = -0.675$, using the following equation:

$$\Delta x_3 = -\frac{(m_b + m_w)^2 l^2 g^2 I_w \cos(x_1) \sin(x_1)}{k_1 I_w detD} - k_2(m_b + m_w) lg \sin(x_1)/(k_1 I_w) \tag{16}$$

For the given steady-state roll-angle, the wheel speed error is calculated equal to approx. 7.2×10^3 rad/s, which is confirmed by the results in Fig. 2.

Summarizing the response of the pendulum, it is observed that the controller has poor disturbance rejection properties. In an actual experiment presented in [8], a small error in the pendulum's angle and a subsequent error in the reaction wheel's speed are attributed to the torque applied by the wiring of the motor. Here, the errors in angle and wheel speed are a result of an assumed lateral acceleration disturbance. It is easy to show that if the system is linearised and augmented with an additional integrator for robustness against disturbances, it becomes uncontrollable. This is an inherent characteristic of the controller and corresponds to the physical requirement of applying a constant motor torque to reject any disturbance at zero pendulum angle. This immediately leads to a diverging reaction-wheel speed. Nevertheless, the controller is found to behave in a similar fashion to a motorcycle rider who maintains the necessary roll-angle in order to counteract the tyre-generated roll moment, using a moment induced by the weight of the vehicle. This behaviour can be exploited for automating the control and enhancing the stability of motorcycles. The associated steady-state reaction-wheel speed error is rather significant for the realistic disturbance considered. Combining this with the motorcycle's yaw rate, which has not been accounted for, will result in a gyroscopic pitch moment likely to alter the tyre normal forces and the overall dynamics of the vehicle. Finally, the required torque shown in Fig. 2, reaches up to approx. 300 Nm, a rather unreasonable value for a small actuator. It should be noted that both the wheel-speed error and the torque are mainly governed by the required bandwidth/stability of the system and only minor improvements have been possible using optimal linear control. These issues are looked at in the remainder of the paper, with the integration of the controller with a motorcycle model.

3. THE MOTORCYCLE MODEL

The motorcycle model is developed in Matlab/Simulink®. It is a fully non-linear model incorporating a total of 12 DOF including the rotation of the reaction wheel. The model does not include frame flexibilities, or rider lateral/lean motion, in accord with the model presented in [2]. These additions are shown to be important [4], [5], but their omission at this stage is not thought to affect the main findings.

3.1 Primary Dynamics

A layout of the motorcycle with some basic dimensions is provided in Fig. 3. The model is set-up around a principal rigid body, comprising the mainframe, engine and rider. This body possesses six DOF, including three translations and three rotations along and about the axes of the local SAE frame, also shown in Fig. 3. The front sub-frame is attached to the main body via a revolute joint along the steering axis. The front suspension fork is allowed to move up/down with the front wheel. The rear suspension arm is connected to the mainframe via a revolute joint. Both wheels are connected to their corresponding suspensions via revolute joints and are allowed to rotate about their spin axes. The reaction wheel is located under the fuel tank with its centre coinciding with the centre of mass (*C.o.M.*) and its spin-axis parallel to the x-axis of the mainframe.

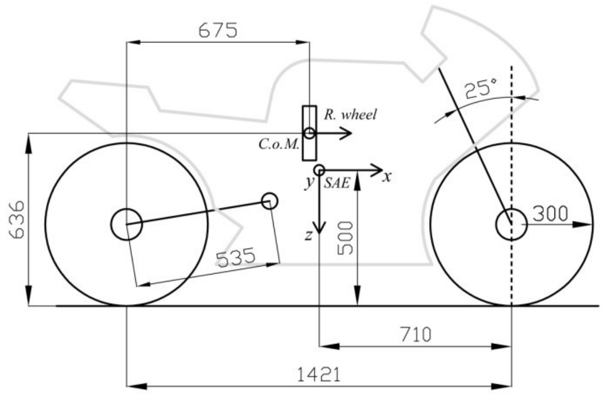

Fig. 3 The motorcycle with basic geometrical properties. All dimensions are in mm

In order to maintain a manageable number of equations, the derivation is based on a Lagrange formulation that neglects constraint equations and the resulting multipliers, i.e. the reaction forces are accounted for in an implicit manner. The Lagrange formulation is as follows:

$$\frac{d}{dt}\frac{\partial T}{\partial \dot{q}_i} - \frac{\partial T}{\partial q_i} + \frac{\partial U}{\partial q_i} = Q_i \qquad (17)$$

where T is the total kinetic energy of the system, U is the potential energy, q_i are the assumed generalized coordinates and Q_i are external forces/moments.

The kinetic energy of the main body is due to its three translational and three angular velocities. The kinetic energy of each subsequent body is a result of the contribution of the velocities of the main body and any additional velocities due to relative motion between the mainframe and that body. For example, the kinetic energy of the front wheel results from a contribution of the six mainframe velocities, the angular velocity of the steering, the translational velocity of the front fork and the angular velocity of the wheel about its spin-axis. Having specified the relevant translational and angular velocities ([u v w] and [p q r]) for an arbitrary body with mass, m_i, and moments/products of inertia I_{xx}, I_{xy}, etc., its kinetic energy is calculated as:

$$\begin{aligned} T_i &= \frac{1}{2} m_i (u^2 + v^2 + w^2) \\ &+ \frac{1}{2}\left(I_{xx} p^2 + I_{yy} q^2 + I_{zz} r^2\right) \\ &- I_{xy} pq - I_{yz} qr - I_{xz} pr \end{aligned} \qquad (18)$$

Applying eq. (17) with local motion variables defined in the moving SAE frame will result in equations of motion that will not hold true for large roll, pitch and yaw angles. In [1], this issue is dealt with by adopting a “modified” Lagrange method, whereby the transformation from global to local variables is performed beforehand and the modified Lagrange equations are written in local generalized coordinates. The same result can be obtained by using local variables in the unmodified eq. (17) and observing that prior to time-differentiation of the scalar momentum terms $\partial T / \partial \dot{q}_i$, scalar momentum entries can be combined to form momentum vectors corresponding to each individual body. Then, it is possible to arrive to the same form of equations as those found in [1] by performing time differentiation using the following operator:

$$\frac{d}{dt} = \frac{D}{Dt}(\,) + \omega \times (\,) \qquad (19)$$

where, ω, corresponds to the angular velocity of the body under consideration and will contain contributions from the rotation of the mainframe and any relevant relative rotations.

The potential energy, U, is a result of suspension spring forces only and gravitational forces/moments are treated as external to the system. The forces/moments, Q_i in (17) are derived using virtual work, taking into consideration all infinitesimal virtual displacements in the direction of the force/moment under examination. Finally, to deal with large angles, the angular velocities transformation presented in [11] is employed. Application of the method results in 12 equations of motion for the motorcycle that can be solved faster than real time in Simulink. The method has been checked against multi-DOF systems with known equations and provides identical formulation of the equations of motion.

3.2 Other Model Attributes

The motorcycle model is coupled with a generic Magic Formula model [1] whereby combined slip is treated using the similarity method [1]. The tyre-road contact is based on a disk-like representation of the tyre, i.e. tyre-width effects are neglected. Tyre width is shown to be an important parameter in [2], [5], however this initial representation is thought to be adequate for the present study. The tyre contact centre moves longitudinally, as a result of steer-angle and body roll.

In terms of rider controls, engine torque is provided by a proportional/integral controller, fed with the forward speed error. Due to the incorporation of the reaction wheel, a roll-angle error feedback to steering torque is not used. Instead, steering torque is provided by a PID controller that acts on steer-angle error. In this manner the steering action is de-coupled from the leaning action.

3.3 Motorcycle Simulation Results

The base-line motorcycle parameters are taken from [2] and correspond to an Aprilia RSV 1000 motorcycle. The main inertia properties are given in Table 1 and the principal dimensions in Fig. 3. The reader is directed to [2] for additional properties.

The 1st simulation involves the controller operating as described in sections 2.1-2.2, i.e. with a steady-state wheel-speed error expected due to the existence of a steady-state roll-angle. The motorcycle travels at 20 m/s and is subjected to a ramp-steer manoeuvre reaching 0.8^{o} of steer-angle in 4 s. The steering controller provides the torque to track this angle. The corresponding response is shown in figures 4-9 and is marked as “0 reference angle” in the labels. Fig. 6 illustrates the expected steady-state error of the reaction wheel speed. In turn, Fig. 7 shows a rather unreasonable power of over 350 kW required from the controller.

The 2nd simulation involves the same steering input and forward speed. In order to eliminate the steady-state error in the reaction wheel speed, a moving roll-angle reference is implemented so that the variable, x_1, in eq. (10), (11), is substituted by:

$$x_1 = x_1 - \frac{1}{\tau s+1}\tan^{-1}\frac{Ur}{g} \tag{20}$$

where, U, is the forward speed, r, is the yaw-rate, g, is the acceleration of gravity and, τ, is a time-constant determining the phase lag with which the steady state roll-angle is applied as a reference angle. Equation (20) effectively makes use of the fact, that, including the steady-state lateral acceleration, Ur, the steady-state roll-angle attained by the motorcycle corresponds to a new unstable equilibrium point.

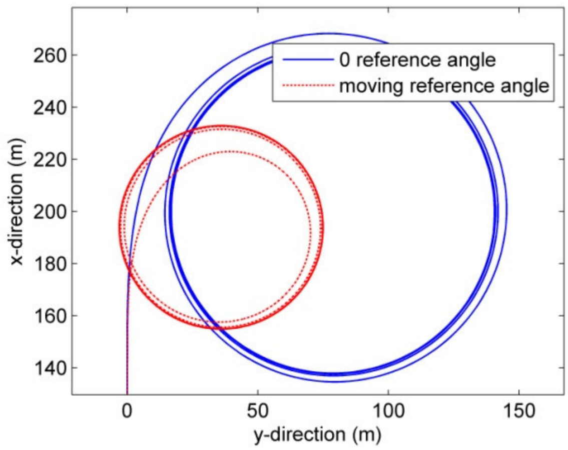

Fig. 4 Motorcycle path

It happens that at steady-state the problem reduces to one described by eq. (1), (2), but with the acceleration of gravity, g, substituted by $g\sqrt{1+(Ur/g)^2}$. This can form the basis for a gain-scheduling-based controller, with Ur/g representing the scheduling variable. For the time being, the non-linear controller developed in 2.1 is maintained and the responses are indicated as “moving reference angle” in the labels in figures 4-9.

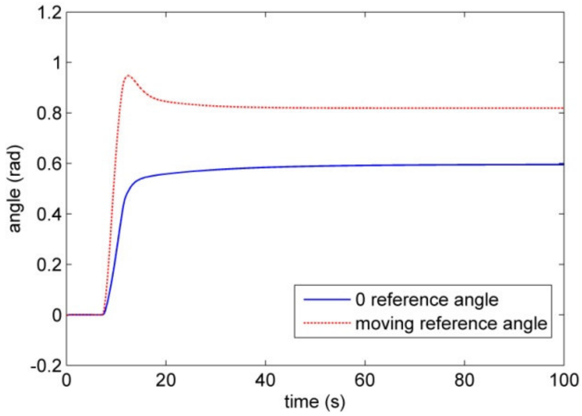

Fig. 5 Motorcycle roll (lean) angle

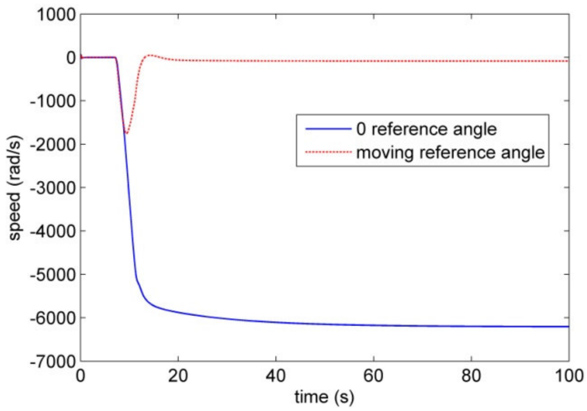

Fig. 6 Reaction wheel angular speed

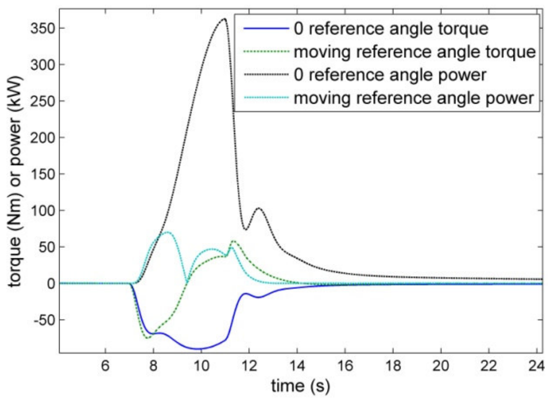

Fig. 7 Controller torque and power

The elimination of the reaction-wheel steady-state speed is shown in Fig. 6. According to Fig. 7, the maximum power has now reduced to 69 kW and the maximum torque is 75 Nm. These values are still impractical. The effort spent by a rider for a similar manoeuvre is significantly less. This is because the controller requires the development of an opposing roll-rate and roll-angle in order to initiate the generation of a stabilizing torque. In reality, the rider makes use of the kinetic energy of the motorcycle by applying opposite-steer [4], thus triggering an initial roll towards the inside of the corner. It is possible that the reaction wheel forms part of an integrated ride-by-wire system, whereby the steering command triggers an initial open-loop sequence where the wheel "throws" the motorcycle to the inside of the corner with little energy expense, prior to the activation of the closed-loop stabilizing control.

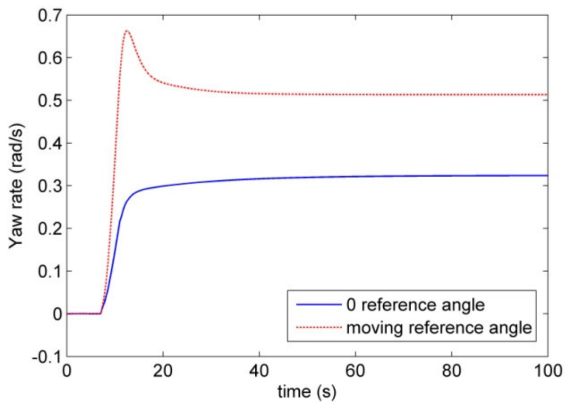

Fig. 8 Motorcycle yaw rate

The gyroscopic weight transfer effects mentioned briefly in section 2.2. are illustrated in Fig. 9. The "0 reference angle" case shows an additional front-to-rear weight transfer of approx. 98 N. Using the motorcycle's global yaw-rate, r, and the wheel's angular rate, $\dot{\varphi}_w$, the pitch moment due to wheel-related gyroscopic effects is calculated as $r\dot{\varphi}_w I_w$, where I_w is the moment of inertia of the reaction wheel about its spin axis. Using the nominal wheelbase of 1.421 m the weight transfer is calculated approx. equal to 90 N. The residual is due to a small track-change, small differences in pitch-angle and other such minor effects.

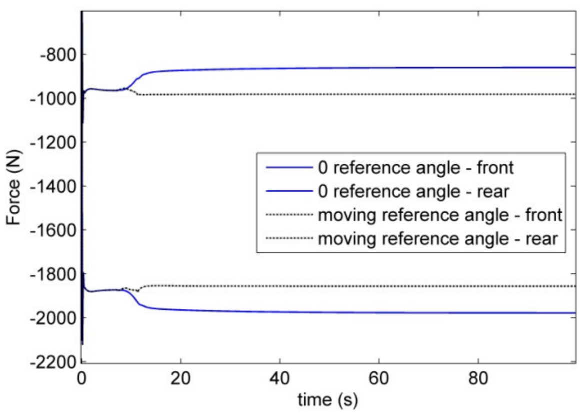

Fig. 9 Tyre normal forces

A final observation refers to the substantially tighter corner described by the motorcycle with moving reference angle, shown in Fig. 4, and the associated increased roll angle and yaw rate in Figs. 5 and 8, respectively. The moving reference angle controller allows the motorcycle to lean more. Due to an exaggerated camber effect and plenty of tyre-force margin in the tyre model, the motorcycle is able to establish a new equilibrium with a significantly increased lateral acceleration. It is expected that a more realistic tyre model will reduce the intensity of this effect.

4. CONCLUSION

The reaction wheel is shown to be able to balance the motorcycle and to relieve the rider from stabilizing the vehicle in roll using steer- or body-lean-torque. The power requirements are found to be unrealistic; however, it appears possible to use the reaction wheel within an integrated ride-by-wire scheme with open-loop elements designed to mimic a rider's actions, thus reducing the required power. With respect to motorcycle modelling, a more representative tyre model will provide more dependable results. Using such a model, further study of the controller is required in order to ascertain its effects on the stability of all the principal modes. Finally, a gain-scheduling controller could be investigated in addition to the feedback-linearisation scheme presented here.

REFERENCES

[1] Pacejka, H. B. "Tyre and Vehicle Dynamics", Butterworth Heinemann, 2006, Oxford.

[2] Cossalter, V. and Lot, R. "A motorcycle Multi-Body Model for Real Time Simulations Based on the Natural Coordinates Approach", *Vehicle System Dynamics*, 2002, 37:6, pp. 423-447.

[3] Cossalter, V., Lot, R. and Maggio, F. "The Modal Analysis of a Motorcycle in Straight Running and on a Curve", *Meccanica*, 2004, 39, pp. 1-16.

[4] Sharp, R. S. "Stability, Control and Steering Responses of Motorcycles", *Vehicle System Dynamics*, 2001, 35:4, pp. 291-318.

[5] Sharp, R. S., Evangelou, S. and Limebeer, D. J. N. "Advances in the Modelling of Motorcycle Dynamics", *Multibody System Dynamics*, 2004, 12, pp. 251-283.

[6] Sharp, R. S. "Motorcycle Steering Control by Road Preview", *ASME Journal of Dynamic Systems, Measurement and Control*, 2007, 129, pp. 373-381.

[7] Oland, E. and Schlanbusch, R. "Reaction Wheel Design for CubeSats", *Proc. Of 4th Int. Conference on Recent Advances in Space Technologies*, 2009, pp. 778-783.

[8] Spong, M. W., Corke, P. and Lozano, R. "Nonlinear control of the Reaction Wheel Pendulum", *Automatica*, 2001, 37, pp. 1845-1851.

[9] Srinivas, K. N. and Behera, L. "Swing-up control strategies for a reaction wheel pendulum", *International Journal of Systems Science*, 2008, 39:12, pp. 1165-1177.

[10] Isidori, A. "Non-linear control systems", Springer, 1995, New York.

[11] Cook, M. V. "Flight Dynamics Principles", Butterworth Heinemann, 1997, Oxford.